

Effect of spatial extension on noise-enhanced phase locking in a leaky integrate-and-fire model of a neuron

Roger Rodriguez^{1,*} and Petr Lánský^{2,†}

¹ *Centre de Physique Théorique, CNRS-Luminy, and Faculté des Sciences de Luminy, Université de la Méditerranée, Case 907, F-13288 Marseille Cedex 09, France*

² *Institute of Physiology, Academy of Sciences of the Czech Republic, Videnská 1083, 142 20 Prague 4, Czech Republic*
(Received 21 July 1999; revised manuscript received 21 June 2000)

Signal transmission enhanced by noise has been recently investigated in detail on the single compartment, also referred to as single point, leaky integrate-and-fire model neuron under a subthreshold stimulation. In this paper we study how this phenomenon is influenced by taking into account the spatial characteristics of the neuron. A stochastic two-point leaky integrate-and-fire model, comprising a dendritic compartment and trigger zone, under periodic stimulation is studied. A method of how to measure synchronization between the signal and the output in both, experiments and models, is proposed. This method is based on a distance between the exact periodic spiking, as expected for sufficiently strong and noiseless stimulation, and neuronal activity evoked by a subthreshold signal corrupted by noise. It is shown that qualitatively the same phenomenon, phase-locking enhanced by the noise, as found in the spatially unstructured neuron is produced by the spatially complex neuron. However, quantitatively there are significant differences. Namely, the two-point model neuron is more robust against the noise and therefore its amplitude has to be higher to enhance the signal. Further, it is found that the range of the critical levels of noise is larger for the two-point model than for the single-point one. Finally, the enhancing effect at the optimal noise is more efficient in the single-point model and thus the firing patterns at their optimal noise levels are different in both models.

PACS number(s): 87.10.+e, 07.05.Mh

I. INTRODUCTION

The single-point models, in which all the properties of a neuron are collapsed into a single point in space, appear, besides the cable models, to be the most common formal description of the neuronal activity [1]. The most frequently applied, studied, modified, and generalized among these models are, as a compromise between tractability and realism, those which are based on the leaky integrate-and-fire (LIF) concept; for a recent review see [2]. The above-mentioned preference of the single-point representation is also obvious in the studies on the stochastic resonancelike phenomena in neuronal models (Refs. [3–14] and many others). A great advantage of the single-point abstraction is its relatively good mathematical tractability and transparency of the achieved results. Another type of approach to the neuronal modeling is based on considering model neurons composed of many compartments (for example, Baldi *et al.* [15] studied a cerebellar Purkyne cell model containing a total of 4550 compartments). These models are investigated mainly by using software packages specifically developed for this purpose [16–18]. The questions posed in these two approaches usually do not overlap. The former one is more oriented on the studies of neuronal functioning in an environment (networks, input-output properties) whereas the latter approach aims at revealing the properties of the neuron itself. The inspiring question for this paper is whether the studies on the input-output characteristics could gain some

new information from such, at least minimal, compartmentalization of a neuron.

A typical neuron has a rather complex anatomical structure. However, at the basic simplification, it can be divided into two distinct parts. It is the dendritic part where the input to the neuron takes place and the trigger zone where the response to the input is generated as the output signal. Of course, in the single-point models these two parts are collapsed into one, despite that their functioning is different. Therefore, several attempts have appeared in the last decade that generalize the single-point models, making them biologically more relevant but still mathematically tractable. Kohn [19] proposed a two-compartment model and similar models were further developed and studied [20–25]. It has been shown in [22,23] that the activity of the two-compartment model is less sensitive to abrupt stimulation changes because these are smoothed out in the transmission from the dendritic compartment to the trigger zone. The delayed response of the two-point model is a consequence of the fact that the input takes place at a compartment different from that at which the output is generated. Further, the model predicts serial correlation of intervals between neuronal firings, interspike intervals (ISIs), which is a phenomenon often observed in experimental data but not reproducible in stochastic single-point models under time-constant input. Finally, as shown in [22], the two-point model neuron is characterized by a lower sensitivity to the input intensity and a larger coding range than the single-point model. All these results were derived for time-constant signals and were based on the assumption that the mean discharge rate is used as the neuronal code. The assumption (implicitly contained in most of the studies on input-output characteristics) is quite realistic because the rate code is one of the basic modes of

*Email address: rodrig@cpt.univ-mrs.fr

†Email address: lansky@sun1.biomed.cas.cz

signaling in the nervous system, for example for the stimulation intensity [26]; as the stimulus intensity is increased, an increase in the neuronal activity is expected to follow almost immediately.

Periodic forces in real neurons come either from the external world in sensory systems or are caused by periodically fluctuating conditions within the neuronal network or, finally, appear within the neuron itself. The sources of periodic stimulation in a model neuron, at least for the LIF model, were studied in [27]. There, the periodic signal, which is influenced by the activity of the neuron under consideration to such an extent that it resets the phase of periodic forcing at each neuronal discharge, is called the endogenous one. The periodic signal which evolves independently of the activity of the studied neuron is called exogenous. There is no doubt about the existence of periodically changing internal conditions in a neuron, but these are not so easy to manipulate experimentally and probably have a smaller effect than externally imposed periodic forces. Due to this limited biological relevance of the endogenous periodicity, and due to the fact that the paper is oriented towards studying the transfer of the external signal by a neuron, here we restrict ourselves to the exogenous periodic input only. A detailed comparison of the effect of noise in dependency on exogenous versus endogenous periodical input in the single-point LIF model was presented recently by Shimokawa *et al.* [12].

The aim of this study is to investigate the effects of periodic stimulation on the simplest spatially structured neuronal model (two point) in comparison with those evoked by the same kind of stimulation applied on the classical nonspatial (single-point) LIF model. At first, the subthreshold properties of the models are summarized. These are necessary for being able to define comparable input signals for both models. Then, a method for measuring the effect of noise on the regularity of firing is proposed. This measure permits us to define an optimal level of the noise enhancing the signal. Further, on the basis of this measure, we conclude that the same effects are present in both models, however, with a substantial quantitative differences: (i) the optimal noise is larger in the two-point model, (ii) the enhancing effect of the optimal noise is weaker in the two-point model than in the single-point one and thus the firing patterns at their optimal noises differ, and (iii) the range of the noise close to the optimum is larger in the two-point model than in the single-point one.

II. THE MODELS

A. Single-point model

In the stochastic LIF model, under a periodic stimulation, the behavior of the membrane depolarization X is described by the stochastic differential equation

$$dX = \left(-\frac{X}{\tau} + \mu + A_1 \cos(\omega t) \right) dt + \sigma_1 dW, \quad (2.1)$$

$$X(t_0) = x_0, \quad t \geq t_0$$

where W is a standard Wiener process, $\tau > 0$ is the membrane time constant ($\tau = RC$, where R is the membrane resistance

and C is its capacitance), μ , A_1 , and $\sigma_1 > 0$ are constants characterizing the input and its variability, t_0 is the moment of the last firing of an action potential, and ω is the frequency of the driving force modulation ($T = 2\pi/\omega$ is the modulation period). The firing of an action potential is identified with the first crossing of X through a firing threshold S , $S > x_0$. At these moments, the membrane potential is repeatedly reset to its initial value x_0 , and for simplicity it is assumed to be equal to zero, $x_0 = 0$. Due to the exogenous character of the signal, the periodic force continues and does not depend on t_0 . The phase-locking effect, in which the neuronal firing synchronizes with the periodical stimulation, has been both theoretically [in Eq. (2.1) using the deterministic signal characterized by $\sigma_1 = 0$] and experimentally (activating a neuron by periodically changing intensity of stimulus) investigated for quite a long time (e.g., [28–31] and many others). Again, mainly the models based on the LIF concept were used for this purpose, but in the deterministic versions.

For studying the model (2.1), three parametric regions may be defined: (1) the permanent suprathreshold in which the constant part of stimulation is sufficient to reach the threshold, (2) the permanent subthreshold in which, whatever is the frequency ω , no sustained firing exists and only a transient activity may appear at the onset of stimulation, and (3) mixed, in which the periodic component determines if the threshold is or is not reachable. For the mean of X in the absence of threshold and under the condition $t_0 = 0$, holds

$$E(X(t)) = \tau \left[\mu(1 - e^{-t/\tau}) + \frac{A_1}{1 + (\omega\tau)^2} \times \left(\frac{\cos(\omega t)}{\tau} + \omega \sin(\omega t) - e^{-t/\tau} \right) \right]. \quad (2.2)$$

The subthreshold stimulation occurs when $\max\{E(X(t)) | t > 0\} < S$, which implies

$$\tau \left(\mu + \frac{A_1}{\sqrt{1 + (\omega\tau)^2}} \right) < S. \quad (2.3)$$

The stimulation is of permanent subthreshold type if $\tau(\mu + A_1) < S$, of permanent suprathreshold type if $\tau\mu > S$, and the mixed cases cover the remaining part of the $\{\mu, A_1\}$ space. In these mixed cases, the value of stimulation frequency ω decides whether the stimulation is actually suprathreshold or subthreshold.

B. Two-point model

The stochastic process X , defined in Eq. (2.1), represents the membrane depolarization at an abstract point of a neuron, which is generally identified with the trigger zone. However, the input, which takes place mainly at the dendritic part of the neuron, is also represented here. This concentration of all properties into the single point is the source of uncertainty of the single-point models. Thus, the description by X is, in the two-point model, replaced by a couple $\{X_1, X_2\}$ representing depolarization in the two distinct parts. The model we analyze here is based on the following set of hypotheses.

(i) The neuron is assumed to be made of two interconnected—dendritic and trigger zone—compartments.

(ii) The stochastic input is present at the dendritic compartment only.

(iii) The potentials of the two compartments are described by leaky integrators with a reset mechanism at the trigger zone.

In the two-point neuronal model, exposed to the same type of input as Eq. (2.1), the depolarization X_1 of the dendritic compartment is defined in the following way:

$$dX_1(t) = \left(-\frac{X_1(t)}{\tau} + \frac{1}{\tau_r} [X_2(t) - X_1(t)] + \nu + A_2 \cos(\omega t) \right) dt + \sigma_2 dW \quad (2.4)$$

and the depolarization X_2 at the trigger zone is

$$dX_2(t) = \left(-\frac{X_2(t)}{\tau} + \frac{1}{\tau_r} [X_1(t) - X_2(t)] \right) dt, \quad (2.5)$$

where τ_r is a junctional time constant; the other parameters have the same interpretation as in Eq. (2.1). It is assumed in equations (2.4) and (2.5) that the membrane time constants are the same at both compartments, $\tau = \tau_1 = \tau_2$, but this assumption can be easily removed. In accordance with the integrate-to-threshold scenario, in the moment when the depolarization X_2 at the trigger zone reaches the firing threshold S , the value of the process X_2 is reset to zero while the process X_1 continues in its evolution. If the occurrence time of this event is taken as the time origin, then the ISI is the first-passage time across the boundary S for X_2 under the initial conditions $X_1(t_0) = x_{10}$ and $X_2(t_0) = 0$, where x_{10} is the value of the dendritic potential at the moment of the last spike. For the deterministic input ($\sigma_2 = 0$), the above described model was studied in detail by Bressloff [20].

First, to be able to define the subthreshold stimulation regime in this model, we investigate the means, $m_1(t) = E(X_1(t))$ and $m_2(t) = E(X_2(t))$, in the absence of a threshold. A general formula for the moments of a stochastic process given by linear stochastic differential equations can be applied to Eqs. (2.4) and (2.5) (e.g., [32]). We have

$$\frac{dm_1(t)}{dt} = -\left(\frac{1}{\tau} + \frac{1}{\tau_r} \right) m_1(t) + \frac{1}{\tau_r} m_2(t) + \nu + A_2 \cos(\omega t) \quad (2.6)$$

and

$$\frac{dm_2(t)}{dt} = -\left(\frac{1}{\tau} + \frac{1}{\tau_r} \right) m_2(t) + \frac{1}{\tau_r} m_1(t). \quad (2.7)$$

For defining subthreshold or suprathreshold parametric regions, we are interested only in the behavior of the moments for large t and thus we will use the initial conditions $m_1(0) = m_2(0) = 0$. The solutions of the above equations are given by

$$m_1(t) = k_1 + k_2 \exp\left(-\frac{1}{\tau} t\right) + k_3 \exp\left[-\left(\frac{2}{\tau_r} + \frac{1}{\tau}\right) t\right] + k_4 \cos(\omega t) + k_5 \sin(\omega t) \quad (2.8)$$

and

$$m_2(t) = l_1 + l_2 \exp\left(-\frac{1}{\tau} t\right) + l_3 \exp\left[-\left(\frac{2}{\tau_r} + \frac{1}{\tau}\right) t\right] + l_4 \cos(\omega t) + l_5 \sin(\omega t), \quad (2.9)$$

where

$$l_1 = \frac{\nu \tau^2}{\tau_r + 2\tau} \text{ and } k_1 = \nu \tau - l_1, \quad (2.10)$$

$$l_2 = -\frac{\tau[\nu + A_2 + \nu(\tau\omega)^2]}{2[1 + (\tau\omega)^2]} = k_2, \quad (2.11)$$

$$l_3 = \frac{\tau\tau_r[(\tau_r + 2\tau)^2(\nu + A_2) - \nu(\tau\tau_r\omega)^2]}{2[(\tau_r + 2\tau)^2 + (\tau\tau_r\omega)^2](\tau_r + 2\tau)} = -k_3, \quad (2.12)$$

$$l_4 = \frac{A_2}{2} \left(\frac{\tau}{1 + (\tau\omega)^2} - \frac{\tau\tau_r}{(\tau_r + 2\tau)^2 + (\tau\tau_r\omega)^2} \right),$$

$$k_4 = \frac{A_2 \tau}{1 + (\tau\omega)^2} - l_4, \quad (2.13)$$

and

$$l_5 = \frac{A_2 \omega}{2} \left(\frac{\tau^2}{1 + (\tau\omega)^2} - \frac{(\tau\tau_r)^2}{(\tau_r + 2\tau)^2 + (\tau\tau_r\omega)^2} \right),$$

$$k_5 = \frac{A_2 \omega \tau^2}{1 + (\tau\omega)^2} - l_5. \quad (2.14)$$

When comparing the means of the two- and single-point models, Eqs. (2.8) and (2.9) with Eq. (2.2), we have $E(X(t)) = m_1(t) + m_2(t)$. The rest of the properties is a direct consequence of this one. The same periodicity is retained in both compartments and also the same decay of the amplitude with increasing frequency of stimulation. For large t we have

$$m_1(t) = k_1 + \sqrt{k_4^2 + k_5^2} \cos(\omega t - \phi_1) \quad (2.15)$$

and

$$m_2(t) = l_1 + \sqrt{l_4^2 + l_5^2} \cos(\omega t - \phi_2), \quad (2.16)$$

where $\text{tg } \phi_1 = k_5/k_4$ and $\text{tg } \phi_2 = l_5/l_4$. By taking different initial conditions, only ϕ_1 and ϕ_2 change. Thus, the division of the input parametric space analogous to that based on Eq. (2.3), which holds for the single-point model, follows from $\max[m_2(t)|t > 0] < S$, namely,

$$l_1 + \sqrt{l_4^2 + l_5^2} < S, \quad (2.17)$$

which defines the permanent subthreshold stimulation.

The equations similar to those for the first moments can be written for the second-order moments. Solving them, the variances of the membrane potential at both compartments and the covariance between them can be computed, see [23]. The relation between the variances is

$$\begin{aligned} \text{Var}(X_2(t)) = & \text{Var}(X_1(t)) - \frac{\tau\tau_r\sigma_2^2}{2(\tau+\tau_r)} \\ & - \left(\text{Var}(X_1(0)) + \frac{\tau\tau_r\sigma_2^2}{2(\tau+\tau_r)} \right) e^{-2\tau\tau_r t/(\tau+\tau_r)} \end{aligned} \quad (2.18)$$

and as pointed out in the cited paper, the second-order moments do not depend on the deterministic part of the signal but only on the noise, and thus they are the same as if $\mu = \nu = A_1 = A_2 = 0$. As we are more interested in the behavior of the trigger zone compartment for its possible comparison with the single-point model than in the dendritic compartment, let us also present the asymptotic form of the autocovariance function $R_2(s, t)$ of X_2 , for large t and s . Let $t \rightarrow \infty$ and $s \rightarrow \infty$, then the autocovariance function depends only on the difference of these two times and for $u = |t - s|$, we have

$$R_2(u) = \frac{\sigma_2^2}{8\tau_r} \left(\frac{\tau^2\tau_r e^{-u/\tau}}{\tau+\tau_r} - \frac{\tau^2\tau_r^2 e^{-(2\tau+\tau_r)u/(\tau\tau_r)}}{(2\tau+\tau_r)(\tau+\tau_r)} \right). \quad (2.19)$$

C. Adjustment of the parameters

Two kinds of parameters appear or are connected to Eq. (2.1); the intrinsic parameters S and τ , which are independent of the input, and the parameters μ , A_1 , ω , and σ_1 , reflecting the input [23,33]. We may regard μ as a background (steady-state) level of the signal A_1 as its time-variable component controlled by ω and σ_1 as the amplitude of the noise. An additional parameter τ_r appearing in Eqs. (2.4) and (2.5) can be classified as the intrinsic parameter, the remaining parameters have the same interpretation as in the single-point model.

An example of system highly sensitive to periodic stimuli are the olfactory neurons [34]. The critical region for these fluctuations is between 1 and 10 Hz, up to 40 Hz in some other systems. Therefore, the range for realistic ω in the models is well specified. Also the intrinsic parameters of the neurons are relatively well known, the firing threshold S ranges from 5 to 15 mV and the time constant τ from 5 to 20 ms. Note that the time constant is sufficiently shorter than the period of stimulation and thus even within one stimulation cycle the depolarization gets close to its steady-state level (if the firing threshold does not prevent it) and thus for suprathreshold stimulation the phase locking in which there is only one spike per several stimulation period is rarely observed. A slightly different situation concerns τ_r because the identification of this parameter may require us to take into account, in addition to electrical properties, the distance between the compartments. To be specific, τ_r has been chosen of the same order of magnitude as τ . The attempts to specify the values of the remaining input parameters are more complicated. Even in the case of direct external stimulation, the input parameters do not reflect the physical levels of stimuli, but rather their transformation into the internal representation (for a more detailed discussion see [23]). There is no possibility of directly measuring the values of μ , A_1 , and σ_1 and an analogous statement holds for the corresponding param-

eters of the two-point model. All these parameters have to be estimated from the spiking activity and the task is of substantial complexity even for the Ornstein-Uhlenbeck model [35,36]. Therefore, their specifications in modeling studies have usually a speculative character.

As mentioned above, and investigated in [22] for the constant inputs, in order to compare the single- and two-point models, their parameters have to be adjusted. To make the same steady-state levels of depolarization, for the constant (background) inputs we have to fulfill the condition

$$\frac{\nu}{\mu} = \frac{2\tau + \tau_r}{\tau}, \quad (2.20)$$

from which, and for the given set of intrinsic parameters τ and τ_r , if the input μ to the single-point model is given, the constant input ν to the two-point model can be calculated. Similarly, relating the amplitudes given by Eqs. (2.16) and (2.2),

$$\frac{A_1\tau}{\sqrt{1+(\omega\tau)^2}} = \sqrt{l_4^2 + l_5^2}, \quad (2.21)$$

the value of A_2 can be evaluated (it is contained in l_4 and l_5).

We are not going to adjust the amplitudes of noise as the other input parameters because we will investigate them in their full ranges; however, a preliminary hint about their relationship can be deduced from the behavior of the autocovariance functions. For example, minimizing the difference of areas under the autocovariance function for the single-point model, $R(u) = \sigma_1^2 \tau e^{-u/\tau}/2$, and that given by Eq. (2.19), we obtain that the ratio between the amplitudes of noise σ_2 and σ_1 follows condition (2.20). Another adjustment comes out from comparing the asymptotic variances, $R(0) = R_2(0)$, which implies

$$\frac{\sigma_2}{\sigma_1} = \sqrt{\frac{2(\tau+\tau_r)(2\tau+\tau_r)}{\tau^2}}. \quad (2.22)$$

So, we have several preliminary estimates, Eqs. (2.20)–(2.22), of the ratio between the amplitudes of the noise in the two-point model and the single-point one for achieving their similar behavior.

III. THE RESULTS

A. A measure of the input-output synchronization

Before going into the comparison of the effect of the noise in the two- and single-point models, we have to find a suitable method for this purpose. The method should be independent of the model, preferably easy to establish in experiments and the obtained results should be easy to interpret. First of all, we need to realize what result is expected and on this basis to propose a measure of the deviation caused by the noise. For the suprathreshold stimulation, the ideal result is achieved if the noise is completely eliminated. Then, the neuron fires only as the signal determines. On the other hand, for the subthreshold conditions, there is no output in the absence of noise. Then, the ideal result is achieved if the parameters (in the single-point model μ and A_1) can

be modified in such a way that the signal is at least minimally suprathreshold (increasing the signal) and again by eliminating the noise. As we are interested in the role of the periodic component we keep, for comparison, its amplitude A_1 constant and change the background signal μ to reach the suprathreshold level. Then, we can return to our noisy signal and measure the distance between the ideal output signal and that influenced or enhanced by the noise. The simplest situation arises for the 1:1 phase-locking regime which is considered here; however, the measure we are going to propose can be also generalized for other cases. So, in 1:1 phase-locking (for suprathreshold stimulation in the absence of noise) $ISI = T$, which is the period of stimulation, and a possible measure of the noise-induced cooperative effect (noise-induced distortion in suprathreshold regime), can be taken as

$$\Delta_m = \int_0^\infty |x - T|^m f(x) dx, \quad (3.1)$$

where $m > 0$ is a parameter and f is the ISI probability density. The minimum of Δ_m equal to zero is achieved for regular firing at period T , $f(x) = \delta(x - T)$. For $m = 2$, the relation (3.1) defines the mean-squared distance, however, other values of m can also be considered. It is obvious that Δ_m is less sensitive, especially for large m , to double firings within one stimulation period than to missing one or even worse several periods of stimulation in a row without any spike. If the mean ISI is T and $m = 2$, then Δ_2 gives a variance of ISI, otherwise

$$\Delta_2 = \text{Var}(ISI) + [\text{mean}(ISI) - T]^2, \quad (3.2)$$

which has a very intuitive interpretation (the distance is given by the variability of ISIs and the squared distance between mean ISI and T).

To calculate the values of Δ_m by using Eq. (3.1) requires us to know the ISI density function, or at least for Eq. (3.2) the first two moments of it. Shimokawa *et al.* [11] developed a sophisticated method for the evaluation of the first-passage-time density in the single-point model (2.1) under the exogenous stimulation; however, no such method has been available for the two-point model equations (2.4) and (2.5), and thus, for the sake of equal conditions, we employ a numerical simulation for both models. To estimate Δ_m from simulated (experimentally observed) ISIs we calculate

$$\hat{\Delta}_m = \frac{1}{n} \sum_{i=1}^n |x_i - T|^m, \quad (3.3)$$

where ISIs are denoted by x_i ($i = 1, \dots, n$). The Euler schema with time step 0.005 ms was applied in Eqs. (2.1), (2.4), or (2.5) to calculate the times needed to cross the threshold (half of this step was used to check the reliability of the procedure). We are aware that simulation of the first-passage-time density for stochastic diffusion processes may be unreliable, at least for some parameters (rare crossings caused by low noise); it overestimates the exact first-passage time [37,38]. Therefore, the procedure was checked using the shorter step and very low noise cases were excluded.

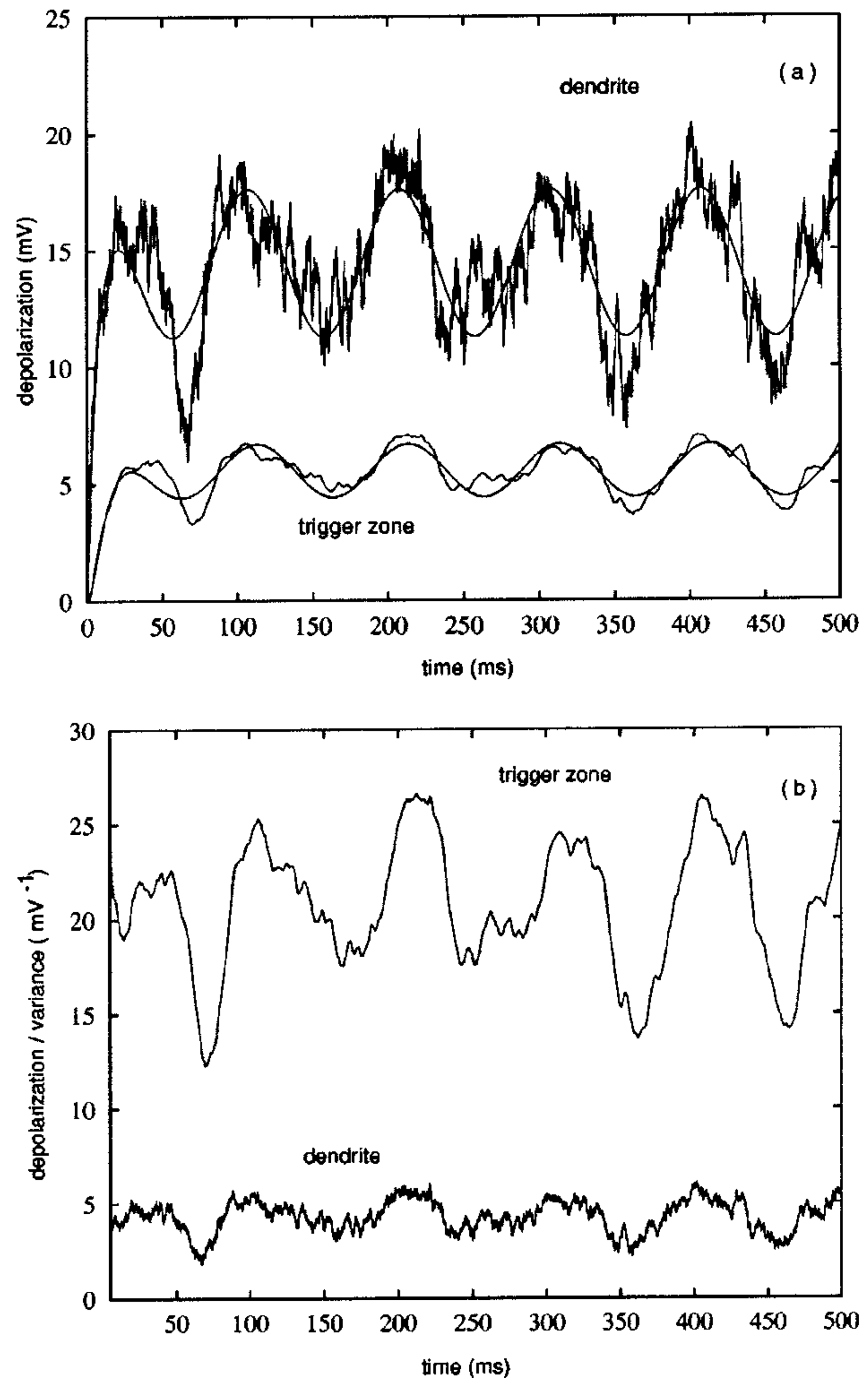


FIG. 1. Behavior of the two-point model with parameters $\nu = 2.1$ mV/ms, $A_2 = 0.5$ mV/ms, $T = 100$ ms, $\sigma_2 = 1$ mV/ $\sqrt{\text{ms}}$, $\tau_r = 16$ ms, $\tau = 10$ ms in the absence of the firing threshold (subthreshold stimulation). (a) The mean depolarizations and single sample trajectories for both compartments. The upper curves are for the dendritic compartment, the lower for the trigger zone. (b) The ratio of the single trajectory of the membrane depolarization to its variance. The upper curve shows the ratio for the trigger zone region while the lower one corresponds to the dendrite.

B. Without firing threshold

The behavior of the two-point model even without imposing a firing threshold reflects well some of its properties. The mean dendritic and trigger zone depolarizations given by Eqs. (2.6) and (2.7) and single trajectories of these depolarizations are illustrated in Fig. 1(a). We can see that the noise is substantially filtered out by the transition from the dendrite to the trigger zone. At the trigger zone, the trajectory follows the mean more closely, while at the dendritic compartment, the noise dominates. The low variability of depolarization at the trigger zone, with respect to the dendritic compartment, follows from formula (2.18), which shows that, rather rapidly, with a time constant $(\tau + \tau_r)/(2\tau\tau_r)$, the steady-state value of the variance of $X_2(t)$ is reached and that it is smaller than the variance of $X_1(t)$. The decrease of the variability level at the trigger zone implies that the relative de-

polarization is higher at the trigger zone than at the dendrite and it is illustrated in Fig. 1(b), where the ratio between a single trajectory of the depolarization and a variance of the depolarization is plotted. We can see that while the trigger zone depolarization is below the dendritic depolarization [see Fig. 1(a)], when related to the variance, it becomes higher. This lower variability at the trigger zone [Fig. 1(a)], reflected also by higher relative depolarization [Fig. 1(b)], suggests robustness of the signal against the noise distortion and/or enhancement present in the two-point model.

C. With firing threshold

1. Suprathreshold stimulation

The simulation of systems (2.4) and (2.5) with an imposed firing threshold is illustrated in Fig. 2. In the noiseless situation ($\sigma_2=0$), the effect of the reset on the behavior of the dendritic compartment is negligible and visible only at the upper phase of stimulation period [Fig. 2(a)]. The phase locking of the firing with the stimulation is apparent in both situations [Fig. 2(a) without noise and Figs. 2(b) and 2(c) with noise]. In Fig. 2(b) and 2(c), again the dendritic depolarization seems to be strongly influenced by the noise and the periodic component is rather hidden in it. On the other hand, the spiking activity looks practically uninfluenced by the noise and preserves the pattern of Fig. 2(a) [see also the corresponding histograms, Figs. 2(d) and 2(e)]. The amplitude of the noise has to be relatively high to destroy the ideal phase-locking effect. Nevertheless, the role of noise can be considered as negative here because it jitters the constant ISIs. In Fig. 2(f) the dependency of $\hat{\Delta}_2$ on the amplitudes of the noise is illustrated. We can see that even here the measure has its meaning starting at zero for the noiseless condition and growing as the jitters of the ISIs increase with the noise. The stronger effect of noise in the single-point model is apparent.

2. Subthreshold stimulation

In Fig. 3 the dependency of $\hat{\Delta}_m$ on the amplitude of noise is presented for different values of m (higher m stresses the importance of missed firings) for the single- and two-point models. We can see in Figs. 3(a), 3(d), and 3(g) that for both models there exist optimal noise levels σ^{opt} determined by the minimum value of $\hat{\Delta}_m$. This optimum is always sharper for the single-point model and it reaches a lower distance from the constant ISI. This is very much apparent in the ISI histograms constructed for the critical noise in both models. For the single-point model [Figs. 3(b), 3(e), and 3(h)] the histograms are better centered around the period of stimulation, however, any small change of the noise amplitude σ_1 would quickly destroy this synchronization. Defining the values of σ as an optimal range of the noise for which the distance $\hat{\Delta}_m$ is not "substantially" different from its minimal value, we can see that the optimal range of σ_2 is larger than that of σ_1 independently of m .

Equations (2.20) and (2.21) relate the input parameters of the single- and two-point models in such a way that the mean depolarizations are the same in both of them. For the parameters selected in Fig. 3 (see the figure legend), the ratio be-

tween ν and μ (between A_2 and A_1) is 3.6 (3.75). As it follows from comparing the autocovariance functions of both models, the value 3.6 would be also the expected ratio between the amplitudes of the critical noise. By using the ratio of asymptotic variances (2.22), the predicted value is 4.33. On the other hand, it follows from the numerical experiment that the ratio between σ_2^{opt} and σ_1^{opt} reaches 10 for $m=2$, 8.12 for $m=1$, and 5.79 for $m=1/2$. The optimal levels of the noise for the two-point model seem to be slightly larger than those suggested by fitting the characteristics like autocovariance or the variances. The reason follows from a lower depth of the profile of the function Δ_m in the two-point cases. It shows that the two-point model cannot reach the quality of the input reproduction whatever is the amplitude of the noise. It means that the ISIs are more scattered around T in the two-point model and in such a case multifiring is preferred over the missed periods.

The bursting (short ISIs) is caused by a higher level of the noise and explains the higher ratio $\sigma_2^{opt}/\sigma_1^{opt}$ than that predicted by the autocovariance functions. The different effect of the noise is well apparent from the ISI histograms [Figs. 3(b), 3(e), and 3(h)] and [Figs. 3(c), 3(f), and 3(i)] which also illustrate the role of parameter m on measure Δ_m . By using larger m (in our case $m=2$), the measure is very sensitive to the long silent periods (long ISIs) and to avoid them in minimizing $\hat{\Delta}_2$, these are eliminated. This, on the other hand, almost completely destroys the phase-locking effect [Fig. 3(c)] and the bursts of more than one spike are typical in this situation. There is another source of bursting, inherent in the two-point model, the positive serial correlation of ISIs, which produces bursting even for constant input [23]. Of course, what value of m is the most appropriate one cannot be answered, but the visual inspection favors Fig. 3(i), which has the ratio of amplitudes of noises close to those predicted by formulas (2.20) and (2.22). As mentioned in Sec. III C 2 the values of Δ_m can be in reality lower than those estimated by $\hat{\Delta}_m$ because of the overestimation of the first-passage time; nevertheless, the shape of the curves would not be different.

Bulsara [39] and Shimokawa [11] measured the input-output enhancement by the height of the ISI density g at T . By using the histograms presented in Fig. 3, we can judge the effect of m on this measure. However, we have to be aware that the amplitudes of noise used in construction of these histograms are optimal with respect to measure Δ but not with respect to the measure $\max\{g(T)\}$. We have for $m=2$: $g_{1p}(100)=265$ and $g_{2p}(100)=87$, for $m=1$: $g_{1p}(100)=345$ and $g_{2p}(100)=229$, for $m=1/2$: $g_{1p}(100)=273$ and $g_{2p}(100)=318$, where the index at g distinguishes the one- or two-point model. We can see that for the single-point model the maximum is reached at $m=1$; however, the peaks of the histograms are rather similar as were the levels of noise deduced for different m . On the contrary, for the two-point model, the maximum is reached at $m=1/2$ and the optimal noise determined by $\max\{g(T)\}$ may be substantially different from that determined by Δ . It follows from comparing the histograms that the firing patterns for the optimal noise are different in both models and also for the two-point model in dependency on m .

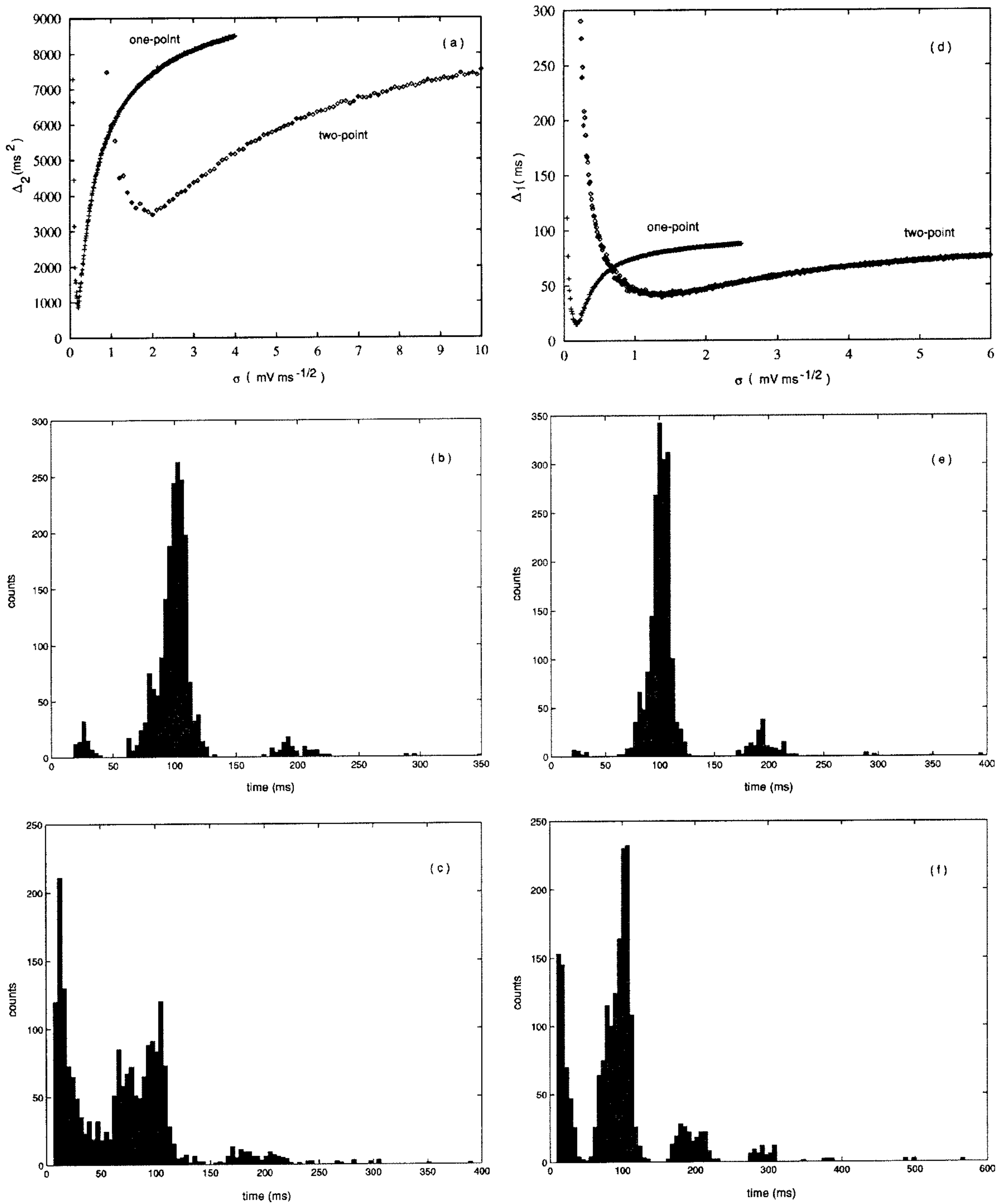


FIG. 3. Dependency of Δ_m on the amplitude of noise in single- and two-point models for subthreshold stimulation and histograms of ISIs for the optimum levels of noise. The parameters of the two-point model are $\nu=2.0$ mV/ms, $A_2=0.5$ mV/ms, $T=100$ ms, $\tau_r=16$ ms, $\tau_2=10$ ms, $S=6.80$ mV, and the corresponding parameters of the single-point model are $\mu=0.556$ mV/ms, $A_1=0.134$ mV/ms; (a) $m=2$, for which the optimal noise is (b) $\sigma_1=0.2$ mV/ $\sqrt{\text{ms}}$, and (c) $\sigma_2=2$ mV/ $\sqrt{\text{ms}}$. In (d) $m=1$, for which the optimal noise is (e) $\sigma_1=0.17$ mV/ $\sqrt{\text{ms}}$, and (f) $\sigma_2=1.38$ mV/ $\sqrt{\text{ms}}$. In (g) $m=1/2$, for which the optimal noise is (h) $\sigma_1=0.19$ mV/ $\sqrt{\text{ms}}$ and (i) $\sigma_2=1.10$ mV/ $\sqrt{\text{ms}}$.

IV. DISCUSSION AND CONCLUSIONS

This study was intended to show the effect of a simple spatial arrangement on the transfer of periodic stimulation by a model neuron. We have seen that by taking into account the distinction between the input site and the output site, all

the properties are qualitatively retained but the quantitative features have dramatically changed. Namely, the optimal level of noise is higher, its effect is not so strong, and the range of noises close to it is broader for the two-point model than for the single-point one. A question may be posed

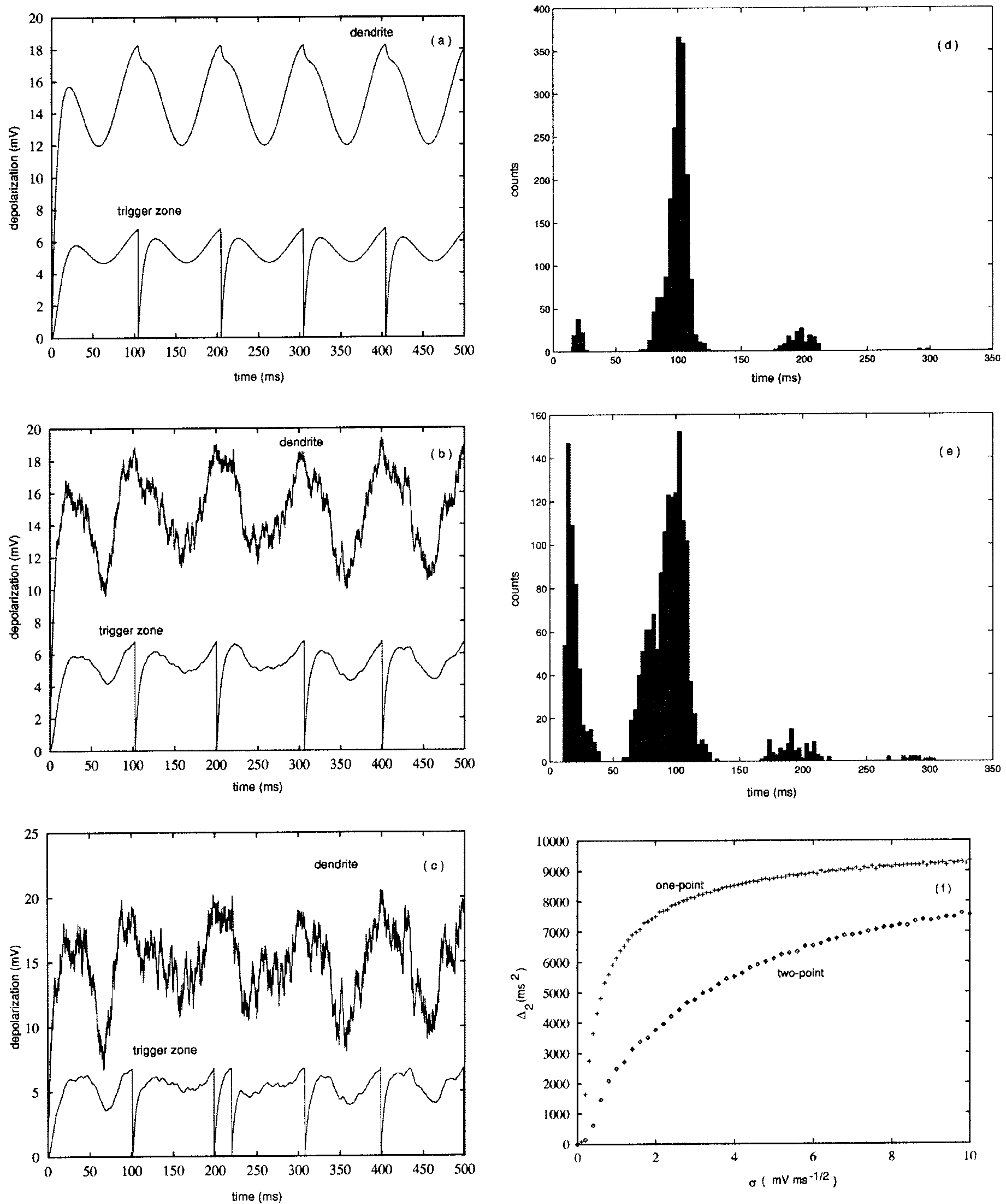


FIG. 2. Simulation of the two-point neuronal model under a suprathreshold stimulation. The variable $X_2(t)$ has been subjected to a reset to 0 at each time the threshold S is reached ($S=6.80$ mV, the rest of the parameters as in Fig. 1). The values of $X_1(t)$ are marginally influenced by the reset. (a) In the absence of noise ($\sigma_2=0$ mV/ $\sqrt{\text{ms}}$), the neuron fires at constant intervals equal to the period of stimulation, $T=100$ ms. (b) and (c) In the presence of noise [$\sigma_2=0.5$ mV/ $\sqrt{\text{ms}}$ and 1 mV/ $\sqrt{\text{ms}}$], the ISIs vary around the period of stimulation, which illustrates the robustness of the trigger zone response (spike generation) to the noise. When noise is acting (with diffusion coefficient $\sigma_2=1$ mV/ $\sqrt{\text{ms}}$, which may be considered as a rather high noise level), the dendrite response to the action of periodic input shows a high variability. On the contrary, at the trigger zone region, the structure of the spiking activity is not fundamentally changed. (d) and (e) Histograms of ISIs for different levels of noise in suprathreshold stimulation ($\sigma_2=0.5$ mV/ $\sqrt{\text{ms}}$; $\sigma_2=1$ mV/ $\sqrt{\text{ms}}$). (f) Dependency of Δ_2 on the amplitude of noise in suprathreshold stimulation for the single-point and two-point models. The parameters for the single-point model are $\mu=0.583$ mV/ms, $A_1=0.134$ mV/ms as follows from Eqs. (2.16) and (2.17). Note the faster growth of the distance for the single-point model.

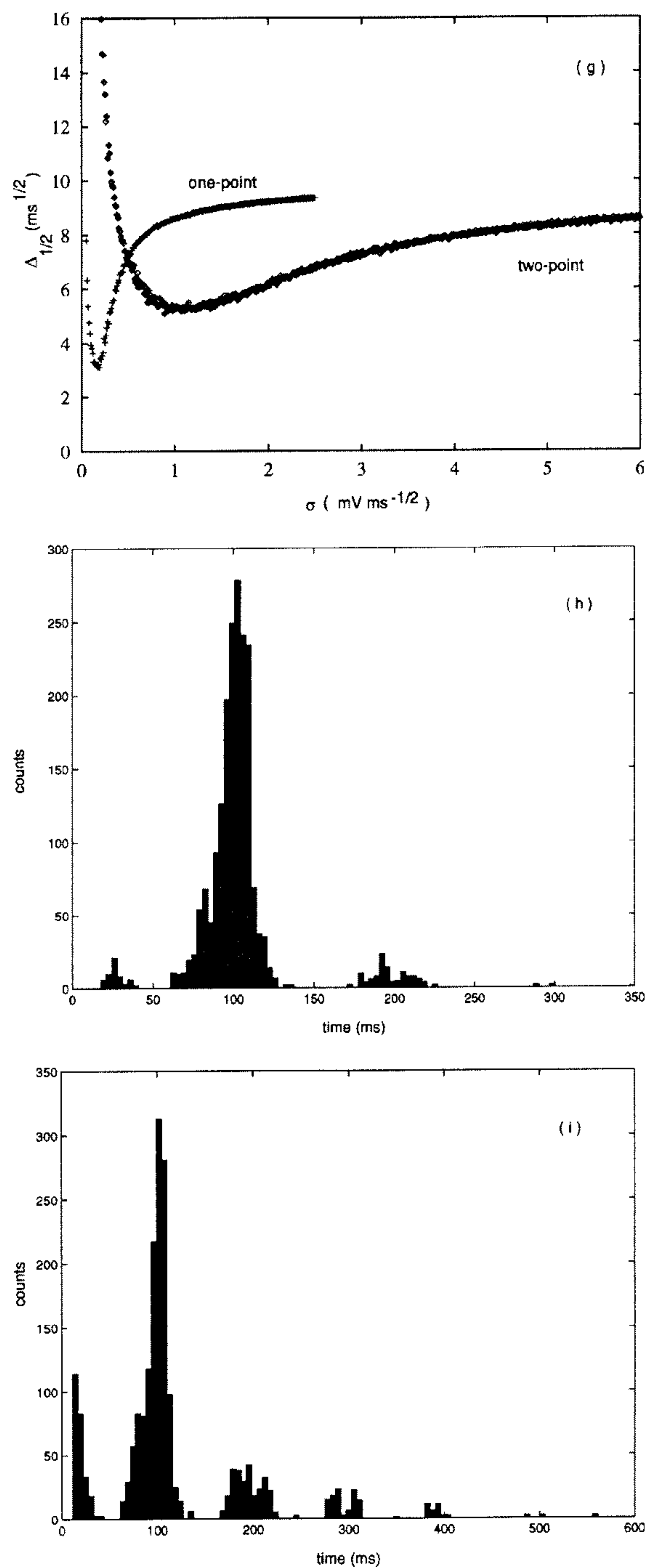


FIG. 3 (Continued).

whether this tendency would continue by higher and higher compartmentalization of the neuron, like the models mentioned in Introduction. The problem has not been investigated here and the answer can be based on an analogy only (some details on the multicompartmental LIF model with white as well as Poissonian noise, but in the absence of periodic stimulation, are presented in [40]). Nevertheless, if the trend observed here by adding more compartments continues, the noise would be finally completely filtered out during

the translation of the signal from the input site to the trigger zone (not only the noise but also the amplitude of the oscillatory part). The measure Δ would be flat. The neuron would fire only as controlled by the background signal or it would remain silent. However, we know that this is not true and several reasons can be offered to explain why. First, the input to the neuron is not located exclusively on the most distal compartment, but all along the neuron. Second, the serial organization of the compartments, implicitly assumed, is not realistic and the branching structure of real neurons can be very complicated. By adding more compartments, even with three units only, a new problem about their different interactions arises. Third, in addition to the external noise, the neuron itself generates its intrinsic noise which can be responsible for signal distortion and/or enhancement. Fourth, the temporal correlation of the inputs, not considered here, may also play its important role in the signal enhancement [41]. Thus, the phenomenon described in this paper (enhancement of the periodic signal by noise) can be expected in the multicompartmental neurons as well. The only, but substantial, problem which remains to be solved is to quantify it properly.

There is a question of whether the difference in the responses of the single-point and two-point models can be eliminated by a proper adjustment of their parameters. Here, we adjust the parameters through the variances and integrated difference between the autocorrelation functions. The rate of the asymptotic decay of the autocorrelation function can also be used. However, there is always a difference between the responses of the models reflected by the qualitatively different behavior of their autocorrelation functions at zero. For the single-point model (the Ornstein-Uhlenbeck process), the autocorrelation function is not differentiable at zero. On the other hand, for the two-point model, the autocorrelation function of the depolarization at the trigger zone is always differentiable, see Eq. (2.19). Thus, whatever parametrization of the models is considered, the single-point model does not behave as a special case of the two-point one.

The problem of the correct specification of the parameters in LIF models of neurons was partly touched here in effort to compare the single-point model with its two-point counterpart. We have not performed a complete parametric study like those presented in the inspiring papers [3,11,12], where are studied the effects of changing the amplitude of the time-varying component of the signal, the background signal, and the stimulation frequency. Additionally, we could ask about the role played by the intrinsic parameters in the enhancement of the signal by noise in both, single- and two-point, models. None of these problems were at the aim of this study, but we only wished to show the effect of spatial arrangement on the information transfer of the periodic signal. For this purpose only one set of parameters was selected, hopefully close to those which can be identified in real neurons. It remains an open question if the ranges of parameters suitable for the enhancement will be changed by compartmentalization.

The measure of the input-output synchronization Δ_m introduced here is easy to interpret (distance to firing at constant frequency) and easy to evaluate from individual ISIs (in the same way as calculating the sample moments). Actually,

it can be evaluated for the majority of already published data giving only average and standard deviation (or coefficient of variation) of ISIs and it is its greatest advantage. As predicted and confirmed by simulation, the measure is rather sensitive, in dependency on m , to the missed periods when no spike is elicited and different values of m can be also interpreted in coding terminology. This sensitivity to missed firing periods seems to be important for the single neuron coding, when the message at the next level of the neuronal network strongly depends on the activity of a single unit. For population coding, in which a large number of neurons converge to a single one (for example, in the olfactory sensory system [42], a missed firing is easily replaced by firing of other source neurons [13]. This distinction can give a hint about the applicability of the measure Δ_m . The other extreme to missed periods is the firing of several spikes, a burst of spikes, not very much separated, during one period of stimulation. In such a case, if the burst is declared as a single complex spike, the phenomenon may be considered as favorable for retaining periodicity in the signal transmission. Then, the measures of the enhancement should take this into account, but both these situations (missed periods and bursts) should be first carefully studied in the single-point model not by simulation but by more reliable (analytical and numerical) methods.

There exist other measures of synchronization by noise of the output with periodic stimulation. The traditional one, in theoretical as well as experimental studies on phase locking, is based on the cycle histograms presenting the spike appearance with respect to the phase of the driving force (see, e.g., [28,43,44]). Using this method, the interspike intervals are converted mod $2\pi/\omega$ so they fall within the interval of one period of stimulation. This method stresses the synchronization over the exact phase locking. In other words, a spike fired after a long period of silence has the same effect, if well synchronized with the signal, as the spike fired during the first period after the reset. We have not applied this method for the comparison of the single- and two-point models as the expected optimum noise levels achieved by this method are low (waiting for a spike can be long) and simulation may introduce substantial distortion of the results. Nevertheless, due to the filtering effect of the compartmental structure of the two-point model we may expect an analogous shift to higher noise amplitude here as well as in any other method.

In [3] and for the sake of comparison also in [11], the measure of the role of noise was based on the comparison of values of the ISI probability density g at the value T (the period of stimulation) in dependency on σ_1 . The critical noise was declared to be that which reached the maxima at $g(T)$ and this method was also applied previously for the simplified LIF (perfect integrate-and-fire) model [4]. This method, as well as that one proposed in this paper, has its advantages and disadvantages and they are partly compared in Sec. III. Again, as in comparison with the cycle-time histogram, the distance (3.1), namely for large m , is very sensitive to higher harmonic firings (with periods $2T$ or more - missing firings), but the maxima of $g(T)$ takes into account the spread of the distribution only marginally (bursting and long ISI have the same effect). Nevertheless, in both measures the understanding of the term "optimal" noise for exogenous stimulation is the same, being based on matching

the stimulation period with the highest rate of firing at this frequency. From the methodological point of view, the numerical evaluation of the first-passage-time density is more difficult than simple simulation of ISIs.

Plesser and Tanaka [10] examined the response of the single-point LIF model to endogenous periodical stimulation. They used for this purpose the most common measure of stochastic resonance—the signal-to-noise ratio (SNR) defined as the ratio of the peak, located at the signal frequency, of the output power spectrum to its background level. The same method was applied by Chapeau-Blondeau *et al.* [45] for the single-point LIF model analogous to Eq. (2.1) in which the periodic component consisted of input pulses received at constant intervals (periodic clicks) corrupted by a Poissonian noise. However, the exogenous periodicity violates the renewal character of the output. Further, the two-point model has nonrenewal output even under the constant conditions being characterized by positive serial correlations of ISIs. This lack of renewal character partly handicaps this method [39] and its extension for exogenous periodicity in the LIF model was proposed only recently [12,46]. Similarly, an assumption that the output is in accordance with an inhomogeneous Poisson process permits us to transform the cycle histogram to the frequency domain and to use the standard SNR measure [13]. A great advantage of the SNR quantification is the knowledge of the formula relating analytically this ratio to the input signal strength, the noise intensity, and the threshold (e.g., [47]). It remains as an open problem to derive a similar formula for measure Δ_m . Especially for $m=2$, the task may be tractable due to relationship (3.2) between Δ_2 and the first two moments of the ISI distribution. There are other measures to evaluate the effect of noise on signal transmission between neuronal input and output. The information-theory based measures were used in [6,39]. Actually, the information transfer in dependency on the variability and correlation structure of ISIs, but irrespectively of the mechanism of their generation, was investigated already more than 30 years ago [48]. A measure based on Fisher information was proposed by Stemmler [14] and for it a relationship analogous to that based on SNR [47] was derived. Another criteria can be based on correlation or coherence between the input and output (e.g., [49]) and undoubtedly others can be found and proposed. Apparently, there is a complete range of methods for quantification of the noise effect in signal transmission and the choice must depend on the purpose, conditions, and interpretability of the results.

We have shown that the general features of the LIF model are also preserved if its spatial version is considered. The results suggest that the suitable levels of the noise may be substantially higher in real neurons than those predicted by the single-point models. And finally, the range of optimal noise may be in reality quite broad, which would prove a relatively high reliability of the neuronal information transfer.

ACKNOWLEDGMENTS

Research was supported by Grant No. A7011712/1997 and by GIS "Sciences de la Cognition" Grant No. CNA 10. We thank C. E. Smith for careful reading of the manuscript and for many stimulating comments.

- [1] H. C. Tuckwell, *Introduction to Theoretical Neurobiology* (Cambridge University Press, Cambridge, 1988).
- [2] P. Lánský and S. Sato, *J. Peripher Nerv. Syst.* **4**, 27 (1999).
- [3] A. R. Bulsara, T. C. Elston, C. R. Doering, S. B. Lowen, and K. Lindberg, *Phys. Rev. E* **53**, 3958 (1996).
- [4] A. R. Bulsara, S. B. Lowen, and C. D. Rees, *Phys. Rev. E* **49**, 4989 (1994).
- [5] A. Capurro, K. Pakdaman, T. Nomura, and S. Sato, *Phys. Rev. E* **58**, 4820 (1998).
- [6] G. Deco and B. Schürmann, *Physica D* **117**, 276 (1998).
- [7] A. Longtin, A. Bulsara, D. Pierson, and F. Moss, *Biol. Cybern.* **70**, 569 (1994).
- [8] G. Mato, *Phys. Rev. E* **58**, 876 (1998).
- [9] Proceedings of the NATO ARW on Stochastic Resonance in Physics and Biology, edited by F. Moss, A. Bulsara, and M. F. Shlesinger [*J. Stat. Phys.* **70**, 1, (1993)].
- [10] H. E. Plesser and S. Tanaka, *Phys. Lett. A* **225**, 228 (1997).
- [11] T. Shimokawa, K. Pakdaman, and S. Sato, *Phys. Rev. E* **59**, 3427 (1999).
- [12] T. Shimokawa, K. Pakdaman, and S. Sato, *Phys. Rev. E* **59**, R33 (1999).
- [13] T. Shimokawa, A. Rogel, K. Pakdaman, and S. Sato, *Phys. Rev. E* **59**, 3461 (1999).
- [14] M. Stemmler, *Network* **7**, 687 (1996).
- [15] P. Baldi, M. C. Vanier, and J. M. Bower, *J. Comput. Neurosci.* **5**, 285 (1998).
- [16] E. De Schutter, *TINS* **15**, 462 (1992).
- [17] I. Segev, *TINS* **15**, 414 (1992).
- [18] I. Segev, J.W. Fleshman, and R.E. Burke, in *Methods in Neuronal Modeling*, edited by C. Koch and I. Segev (MIT Press, Cambridge, 1989).
- [19] A. F. Kohn, *IEEE Trans. Biomed. Eng.* **36**, 44 (1989).
- [20] P. C. Bressloff, *Physica D* **80**, 399 (1995).
- [21] P. C. Bressloff and J. G. Taylor, *Neural Networks* **7**, 1153 (1994).
- [22] P. Lánský and R. Rodriguez, *Biol. Cybern.* **81**, 161 (1999).
- [23] P. Lánský and R. Rodriguez, *Physica D* **32**, 267 (1999).
- [24] P. Lánský and J.-P. Rospars, *Biol. Cybern.* **72**, 397 (1995).
- [25] J.-P. Rospars and P. Lánský, *Biol. Cybern.* **69**, 283 (1993).
- [26] E. D. Adrian, *The Basis of Sensation: The Action of the Sense Organs* (W.W. Norton, New York, 1928).
- [27] P. Lánský, *Phys. Rev. E* **55**, 2040 (1997).
- [28] C. Ascoli, M. Barbi, S. Chillemi, and D. Petracchi, *Biophys. J.* **19**, 219 (1977).
- [29] J. P. Keener, F. C. Hoppensteadt, and J. Rinzel, *SIAM (Soc. Ind. Appl. Math.) J. Appl. Math.* **41**, 503 (1981).
- [30] B. W. Knight, *J. Gen. Physiol.* **59**, 734 (1972).
- [31] A. Rescigno, R. B. Stein, R. L. Purple, and R. E. Poppele, *Bull. Math. Biophys.* **32**, 337 (1972).
- [32] L. Arnold, *Stochastic Differential Equations: Theory and Applications* (Wiley, New York, 1974).
- [33] H. C. Tuckwell and W. Richter, *J. Theor. Biol.* **71**, 167 (1978).
- [34] J.-P. Rospars, V. Krivan, and P. Lánský, *Chem. Senses* **25**, 293 (2000).
- [35] J. Inoue, S. Sato, and L. M. Ricciardi, *Biol. Cybern.* **73**, 209 (1995).
- [36] S. Shinomoto, Y. Sakai, and S. Funahashi, *Neural Comput.* **11**, 935 (1999).
- [37] P. Lánský and V. Lánská, *Comput. Biol. Med.* **24**, 91 (1994).
- [38] R. Mannella, *Phys. Lett. A* **254**, 257 (1999).
- [39] A. R. Bulsara, in *Brain-like Computing and Intelligent Information Systems*, edited by N. Kasabov and S. I. Amari (Springer, New York, 1998).
- [40] R. Rodriguez and P. Lánský, *BioSystems* (to be published).
- [41] Y. Sakai, S. Funahashi, and S. Shinomoto, *Neural Networks* **12**, 1181 (1999).
- [42] W. van Drongelen, A. Holley, and K. B. Doving, *J. Theor. Biol.* **71**, 39 (1978).
- [43] A. S. French, A. V. Holden, and R. B. Stein, *Kybernetik* **11**, 15 (1972).
- [44] A. R. Palmer and I. J. Russell, *Hear. Res.* **24**, 1 (1986).
- [45] F. Chapeau-Blondeau, X. Godivier, and N. Chambet, *Phys. Rev. E* **53**, 1273 (1996).
- [46] H. E. Plesser and T. Geisel, *Phys. Rev. E* **59**, 7008 (1999).
- [47] K. Wiesenfeld and F. Moss, *Nature (London)* **375**, 33 (1995).
- [48] R. B. Stein, *Biophys. J.* **7**, 797 (1967).
- [49] D. R. Chialvo, A. Longtin, and J. Muller-Gerking, *Phys. Rev. E* **55**, 1798 (1997).